

Mitochondrial DNA abnormalities in skeletal muscle of patients with sporadic amyotrophic lateral sclerosis

Stefan Vielhaber,¹ Dagmar Kunz,⁴ Kirstin Winkler,¹ Falk R. Wiedemann,¹ Elmar Kirches,² Helmut Feistner,¹ Hans-Jochen Heinze,¹ Christian E. Elger,⁵ Walter Schubert³ and Wolfram S. Kunz⁵

¹Department of Neurology, ²Institute of Neuropathology and ³Institute of Medical Neurobiology, University of Magdeburg Medical Center, Magdeburg, ⁴Institute of Clinical Chemistry, Medical Center of RWTH Aachen, Aachen and ⁵Department of Epileptology, University of Bonn Medical Center, Bonn, Germany

Correspondence to: Wolfram S. Kunz, Department of Epileptology, University of Bonn Medical Center, Sigmund-Freud-Str. 25, D-53105 Bonn, Germany
E-mail: kunz@mail.meb.uni-bonn.de

Summary

Amyotrophic lateral sclerosis is a neurodegenerative disease affecting the anterior horn cells of the spinal cord and cortical motor neurons. Previous findings have suggested a specific impairment of mitochondrial function in skeletal muscle of at least a limited number of patients. Applying flavoprotein/NAD(P)H autofluorescence imaging of mitochondrial function in saponin-permeabilized muscle fibres, we detected a heterogeneous distribution of the respiratory chain defect among individual fibres in muscle biopsies of patients (11 out of 17) with sporadic amyotrophic lateral sclerosis (SALS). These findings correlate with the presence of cytochrome *c* oxidase (COX)-negative muscle

fibres detected histologically. We established the molecular basis for the decreased activities of NADH:CoQ oxidoreductase and COX in SALS muscle. In the skeletal muscle of the investigated patients, diminished levels (13 out of 17) or multiple deletions (one out of 17) of mitochondrial DNA (mtDNA) were observed. These alterations of mtDNA seem to be related to decreased levels of membrane-associated mitochondrial Mn-superoxide dismutase. Our results support the viewpoint that an oxygen radical-induced impairment of mtDNA is of pathophysiological significance in the aetiology of at least a subgroup of patients with SALS.

Keywords: sporadic amyotrophic lateral sclerosis; mitochondria; oxidative phosphorylation; mitochondrial DNA damage; oxygen radicals; Mn-SOD

Abbreviations: ALS = amyotrophic lateral sclerosis; COX = cytochrome *c* oxidase; FALS = familial ALS; mtDNA = mitochondrial DNA; NADHTR = nicotinamide adenine dinucleotide (reduced) tetrazolium reductase; rDNA = ribosomal DNA; ROS = reactive oxygen species; SALS = sporadic ALS; SDH = succinate dehydrogenase; SOD = superoxide dismutase

Introduction

Amyotrophic lateral sclerosis (ALS) is a motor neuron disease [incidence 0.4–2/100 000, prevalence 2–6/100 000 (Emery, 1991)] leading to a progressive degeneration of the anterior horn cells of the spinal cord and cortical motor neurons. The aetiology and pathogenesis of the neuronal death in ALS is unknown. Present concepts relate the neurodegenerative process to glutamate-induced excitotoxicity (Ludolph *et al.*, 1987; Spencer *et al.*, 1987; Rothstein *et al.*, 1992), but the direct involvement of glutamate transport is still in dispute (Meyer *et al.*, 1995, 1996).

There seems to be compelling evidence for increased oxygen radical damage in brain tissue of patients with ALS

(Bowling *et al.*, 1993; Beal, 1995). In line with this concept, it was demonstrated that some patients with autosomal-dominant familial ALS (FALS) have point mutations in the CuZn-superoxide dismutase (*SOD1*) gene (Rosen *et al.*, 1993). Mouse models which carry these mutations develop severe motor neuron disease (Chiu *et al.*, 1995; Wong *et al.*, 1995). Interestingly, the most obvious ultrastructural abnormality in these animal models is the presence of vacuoles in axons and dendrites which appear to be derived from degenerating mitochondria (Wong *et al.*, 1995; Mourelatos *et al.*, 1996). Similarly, in anterior horn neurons of patients with sporadic ALS (SALS), conglomerations of

dark abnormal mitochondria have been detected (Sasaki *et al.*, 1996). These findings, suggesting a possible involvement of mitochondria in the process of degeneration of motor neurons, are supported by recent observations that creatine administration, which facilitates the buffering of intracellular energy levels, has neuroprotective effects in transgenic mice carrying the G93A human *SOD1* mutation (Klivenyi *et al.*, 1999). Moreover, a cytochrome *c* oxidase (COX) subunit I microdeletion causing a severe COX deficiency in skeletal muscle of a patient with motor neuron disease has been reported (Comi *et al.*, 1998) and we observed a severe deficiency of NADH:CoQ oxidoreductase in skeletal muscle biopsies of 14 patients with SALS (Wiedemann *et al.*, 1998). In this investigation, we expanded this previous study and established the molecular basis of the respiratory chain defect. We observed that the impairment of mitochondrial function in skeletal muscle of our patients correlated with multiple mitochondrial (mtDNA) deletions or decreased mtDNA levels which are associated with low levels of membrane-associated Mn-SOD.

Subjects and methods

Subjects

We studied 17 patients with SALS (nine female, eight male), age range 40–66 years (median age of onset 56 years). According to the El Escorial criteria (Brooks, 1994), 12 patients had definite and five had probable ALS at time of muscle biopsy. Five patients from the previous study (Wiedemann *et al.*, 1998) were included. The duration of illness was 2–4 years. The muscle biopsy was taken from a clinically minor [grade 4/5 of the British Medical Research Council (BMRC) scale] or unaffected muscle (Mm. vastus lateralis or deltoideus). The EMG examination gave evidence of widespread denervation in muscles of different segmental innervation in all four extremities. Motor nerve conduction studies were either normal or revealed a slight slowing (<80% of the normal values) and decreased compound muscle amplitude compatible with motor neuron disease. Multifocal conduction blocks were excluded. In laboratory studies, cerebrospinal-fluid-associated disorders dysproteinemia, anti-GM₁ antibodies, vasculitis and hexosaminidase A deficiency were ruled out. No patient had a history of prior poliomyelitis, and the antibodies were in the range of a normal population.

Skeletal muscle samples from diagnostic biopsies of 21 neurologically normal patients with questionable myopathic EMG abnormalities but no biopsy evidence for a manifest myopathy were used as controls (age range 38–72 years, median age 54; 11 female, 10 male). Two patients with spinal muscular atrophy (having deletions of exons 7 and 8 in the *telSMN* gene, ages 6 and 18 years, one female, one male) were used as disease controls in the Southern blots presented in Fig. 4 and the SOD determinations in Table 2. All patients gave written informed consent prior to biopsy. The study

was approved by the ethical committee of the University of Magdeburg Medical Centre.

Muscle histology

Serial cryostat sections of fresh frozen tissue were stained with haematoxylin–eosin, oil red O, periodic acid–Schiff, Gomori's trichrome, and for nicotinamide adenine dinucleotide (reduced) tetrazolium reductase (NADHTR), myosin adenosine triphosphatase (ATPase) at pH 4.2, 4.6 and 9.4, COX and succinate dehydrogenase (SDH). Consecutive cryostat sections (6 µm) of muscle biopsies from SALS patients were correlated for histochemical mitochondrial stains (COX, NADHTR and SDH). The protocols for these reactions are given in references describing routine muscle biopsy (Dubowitz and Brooke, 1973).

Preparation of muscle fibres

About 50 mg of biopsy tissue was used for isolation of saponin-permeabilized fibres. Bundles of muscle fibres usually containing two to four single fibres were isolated by mechanical dissection. The saponin treatment was performed by incubation of the fibre bundles in relaxing solution (for composition, see below) containing 50 µg/ml saponin as described by Kunz and colleagues (Kunz *et al.*, 1993). The relaxing solution contained 10 mM Ca/CaEGTA buffer (free concentration of calcium 0.1 µM), 20 mM imidazole, 20 mM taurine, 49 mM K-MES (2-[*N*-morpholino]ethane sulphonic acid), 3 mM KH₂PO₄, 9.5 mM MgCl₂, 5 mM ATP, 15 mM phosphocreatine, pH 7.1. The measurements were performed in a medium consisting of 110 mM mannitol, 60 mM KCl, 10 mM KH₂PO₄, 5 mM MgCl₂, 0.5 mM Na₂EDTA and 60 mM Tris–HCl, pH 7.4.

Enzyme activities

The activity of COX was measured spectrophotometrically in 100 mM phosphate buffer, pH 7.4, in the presence of 0.1% laurylmaltoside and 200 µM cytochrome *c*. To measure this high cytochrome *c* concentration, we used a dual-wavelength photometer (Aminco DW 2000, SLM Instruments, Rochester, NY, USA) and worked in the β-band of ferrocycytochrome *c* (510–535 nm; $\epsilon_{\text{red-ox}} = 5.9 \text{ mM}^{-1} \text{ cm}^{-1}$). The activities of NADH:cytochrome *c* and succinate: cytochrome *c* oxidoreductases were measured in 100 mM phosphate buffer (pH 7.4) containing 1 mM KCN, 10 mM NADH or 20 mM succinate and 80 µM ferricytochrome *c* at 550 nm. The activities of lactate dehydrogenase, adenylate kinase, creatine kinase, aspartate aminotransferase and citrate synthase were determined by standard methods as described by Bergmeyer (Bergmeyer, 1970). The maximal glutamate + malate and succinate oxidation rates of saponin-permeabilized muscle fibres were determined as previously described (Kunz *et al.*, 1993).

Fluorescence microscopy of isolated muscle fibres

The isolated fibres were fixed at both ends on a coverslip in a Heraeus flexiperm chamber (Hanau, Germany) and incubated in the medium for measurements. The digital video images were acquired with an inverse fluorescence microscope (model IX-70; Olympus, Tokyo, Japan) equipped with a CCD camera (model CF 8/1 DXC; Kappa, Gleichen, Germany). The NAD(P)H fluorescence image was obtained using 366 nm excitation and 450 nm long-path emission, and the flavoprotein fluorescence image was obtained using 470 nm excitation and 525 nm narrow-band emission. The digital ratio images were calculated using LSM software (Carl Zeiss, Jena, Germany).

Southern blots

Total DNA was isolated from 10–40 mg of liquid nitrogen-frozen muscle samples by standard methods and Southern blots were performed with 1 µg of DNA digested with either *PvuII* or a combination of *PvuII* and *BamHI* (Sambrook *et al.*, 1989). Human skeletal muscle mtDNA and a cloned fragment of the human 18S rRNA gene (a kind gift of Dr C. McMillan, Montreal, Canada) were labelled with digoxigenin by the Klenow reaction. Either mtDNA or a mixture of both labelled DNAs was used to hybridize to the Southern blots as indicated. Blots were developed by CSPD-chemiluminescence (TROPIX). In *PvuII*-digested human DNA, the probe mixture bound to a 16.6 kb mtDNA band and a 12.0 kb chromosomal reference band containing the multicopy 18S rRNA gene. Test blots with various concentrations of both labelled components were performed. We attempted to find the ratio of the two probes which resulted in comparable signal intensities of mitochondrial and chromosomal reference bands using a large number of control DNAs. Southern blots containing DNA from the SALS patients and control subjects were hybridized with aliquots containing the same mixture of probes. For the quantitative determination of the mtDNA/18S ribosomal DNA (rDNA) ratio, ³²P-labelled probes were used. The measurement of the amounts of hybridized probes was performed applying a phosphorimager (Fujix BAS-1000, Fuji PhotoFilm Co., Tokyo, Japan).

Determination of SOD levels

The levels of CuZn- and Mn-SOD in muscle sample fractions were determined with commercially available ELISA (enzyme-linked immunosorbent assay) kits according to the manufacturer's instructions. The ELISA for human CuZn-SOD was purchased from Bender MedSystems (Vienna, Austria) and that for human Mn-SOD from Sceti Co., Ltd (Tokyo, Japan). The frozen muscle samples were homogenized at 50 mg wet weight per ml in 0.1 M phosphate buffer, pH 7.4, with an ultra-turrax homogenizer (IKA, Staufen, Germany) and centrifuged for 10 min at 14 000 r.p.m. in a refrigerated

Sorvall microfuge. The supernatant contained all cytosolic (100% of lactic dehydrogenase) and nearly all mitochondrial matrix enzymes (85–90% of citrate synthase). The pellet, which contains all mitochondrial inner membrane-associated enzyme activities (100% of COX), was resuspended in half of the volume of the added homogenization buffer and kept frozen until use.

Statistical analysis

All enzyme activities are expressed as means ± standard deviation. Statistically significant differences were assessed by the Student's *t*-test. A *P*-value of <0.05 was accepted as the level of significance.

Results

The mitochondrial defect in SALS muscle is distributed heterogeneously

Table 1 gives both mitochondrial and cytosolic enzyme activities as well as respiration rates of saponin-permeabilized fibres from vastus lateralis muscle of the 17 patients with SALS. The activities of the cytosolic enzymes lactic dehydrogenase, adenylate kinase and creatine kinase were normal. In contrast, SALS biopsies had substantially decreased activities of NADH:cytochrome *c* oxidoreductase and COX, whereas citrate synthase and succinate:cytochrome *c* oxidoreductase activities were almost unchanged compared with those of the control group. Additionally, decreased maximal glutamate + malate oxidation rates of saponin-permeabilized muscle fibres were observed. These results suggest a specific impairment of mitochondrially encoded enzymes in SALS muscle, similar to that seen in mtDNA diseases. This is largely in agreement with the results of our earlier report on 14 patients (Wiedemann *et al.*, 1998), five of whom were included in the present study. However, in contrast to our earlier findings, we observed a lower COX activity in this patient group.

The biochemical data were correlated with morphological findings in the biopsies. Histological examination of the skeletal muscle showed, in all cases, characteristic features of neurogenic atrophy including small or larger groups of elongated atrophic muscle fibres, and fibre type grouping in the myosin ATPase reactions (not shown). The percentage of atrophic fibres was never >20%. In no case were inflammatory infiltrates or profound secondary myopathic changes present. In order to examine carefully the subcellular distribution and staining patterns of mitochondria within the muscle fibres, we have correlated NADHTR/SDH reactions with COX enzyme histochemistry. As indicated for a typical patient in Fig. 1, we detected mitochondrial staining abnormalities such as COX-deficient fibres, central and multiple cores or core-like staining defects in the SALS biopsies. The latter were rather frequent (between 1 and 10% of fibres) in seven of the 17 patients. On the other hand, COX-negative fibres were seen at a frequency of 1–2% of

Table 1 Enzyme activities in skeletal muscle and respiration activities of saponin-permeabilized fibres of patients with SALS

Enzyme	Controls (n = 21)	SALS (n = 17)	Significance
Lactate dehydrogenase	286 ± 163	288 ± 155	NS
Adenylate kinase	213 ± 90	276 ± 82	NS
Creatine kinase	1512 ± 398	1780 ± 670	NS
Aspartate aminotransferase	39.3 ± 9.8	39.7 ± 15.3	NS
Citrate synthase	11 ± 2.2	11 ± 3.2	NS
NADH:cytochrome <i>c</i> reductase	3.5 ± 1.7	2.2 ± 1.1	<i>P</i> < 0.01
Succinate:cytochrome <i>c</i> reductase	1.7 ± 0.7	1.6 ± 0.7	NS
Cytochrome <i>c</i> oxidase	7.1 ± 3.5	4.0 ± 2.2	<i>P</i> < 0.01
Glutamate + malate respiration	8.2 ± 0.9	7.2 ± 1.5	<i>P</i> < 0.05
Succinate respiration	10.3 ± 2.1	9.8 ± 3.1	NS

The enzyme activities (in U/g wet weight) were determined at 30°C in the muscle homogenates as described in Subjects and methods. The maximal respiration activities of saponin-permeabilized muscle fibres (expressed in nmol O₂/min/mg dry weight) were determined at 25°C in a medium consisting of 110 mM mannitol, 60 mM KCl, 10 mM KH₂PO₄, 5 mM MgCl₂, 0.5 mM Na₂EDTA, 60 mM Tris-HCl (pH 7.4), 1 mM ADP and 10 mM glutamate + 5 mM malate or 10 mM succinate + 10 μM rotenone, respectively. NS = not significant.

fibres in 11 of the 17 patients. 'Ragged red fibres' or SDH hyper-reactive fibres characteristic of mitochondrial myopathies were found at a very low frequency (0.1 and 0.3% of fibres, respectively) in only one of the 17 investigated SALS biopsies. We also performed a quantitative morphological evaluation of five of our control biopsies (age range 55–60 years). In one of these patients (age 55 years) only we observed a single COX-negative fibre (in the entire biopsy cross-section containing ~1500 single fibres).

Direct correlations of the different mitochondrial stains were performed in consecutive 6 μm cryostat sections. As shown in Fig. 1 (A–C, asterisk) the observed COX-negative fibres showed positive enzyme reactions for NADHTR and SDH. In addition, in some of the SALS biopsies (seven out of 17), muscle fibres were present that showed core-like defects in the COX and SDH reactions, whilst the corresponding NADHTR reaction in the consecutive section showed a normal subcellular enzyme reaction (Fig. 1, A–C, arrow 1). Furthermore, we observed two additional mitochondrial staining types of the core-like defects: COX⁻/SDH⁻/NADHTR⁻ (Fig. 1, A–C, large arrow) and COX⁻/SDH⁺/NADHTR⁻ (Fig. 1, A–C, arrow 2). While the presence of COX-negative fibres is in accordance with the observed changes in mitochondrial enzyme activities in the skeletal muscle homogenates of the SALS patients, these core-like and targetoid changes which do not affect COX exclusively are most likely unspecific changes which are known for denervated fibres (Dubowitz and Brooke, 1973).

To examine further the heterogeneous distribution of the mitochondrial abnormalities within the SALS skeletal muscle samples, we applied an imaging technique which allowed visualization of the defective mitochondrial function within a bundle of muscle fibres (Kuznetsov *et al.*, 1998). For this purpose, we acquired microscopic autofluorescence images

of fluorescent flavoproteins (excitation at 470 nm, emission at 525 nm) and NAD(P)H (excitation at 366 nm, emission at 450 nm) of saponin-permeabilized muscle fibre bundles. The ratio of these different autofluorescence images is a sensitive indicator of a fibre-specific functional impairment of mitochondria, since this indicates rate changes of oxidative phosphorylation (Mayevsky and Chance, 1982; Kuznetsov *et al.*, 1998). Figure 2 shows a typical experiment with an SALS muscle fibre bundle consisting of two muscle fibres. In the endogenous fully oxidized state of both these fibres, the ratio of the autofluorescence images [flavoprotein/NAD(P)H] is high (Fig. 2B). The latter results from the high flavoprotein α-lipoamide dehydrogenase fluorescence in the oxidized state and the low pyridine nucleotide fluorescence. The addition of the mitochondrial substrates octanoylcarnitine and malate caused a partial reduction of the mitochondrial NAD system leading to a darker ratio image (Fig. 2C). Interestingly, one fibre became almost black, while the intensity of the other fibre was only moderately decreased. This indicates rate differences of oxidative phosphorylation in these fibres. Thereafter, we added 1 mM ADP to achieve the maximal stimulation of electron flow through the respiratory chain. Again, the right fibre became brighter, while the other fibre remained in the dark state (Fig. 2D). On addition of cyanide, which selectively blocks COX, the right fibre became dark and the left fibre remained almost unchanged (Fig. 2E). As reported previously (Kuznetsov *et al.*, 1998; Saks *et al.*, 1998), control skeletal muscle fibres show behaviour similar to that of the right muscle fibre. Therefore, this experiment provided strong evidence for a selective inhibition of the respiratory chain which occurred only in the left muscle fibre. We observed these functional heterogeneities detected by the applied imaging technique in the majority of the SALS specimens (11 out of 17).

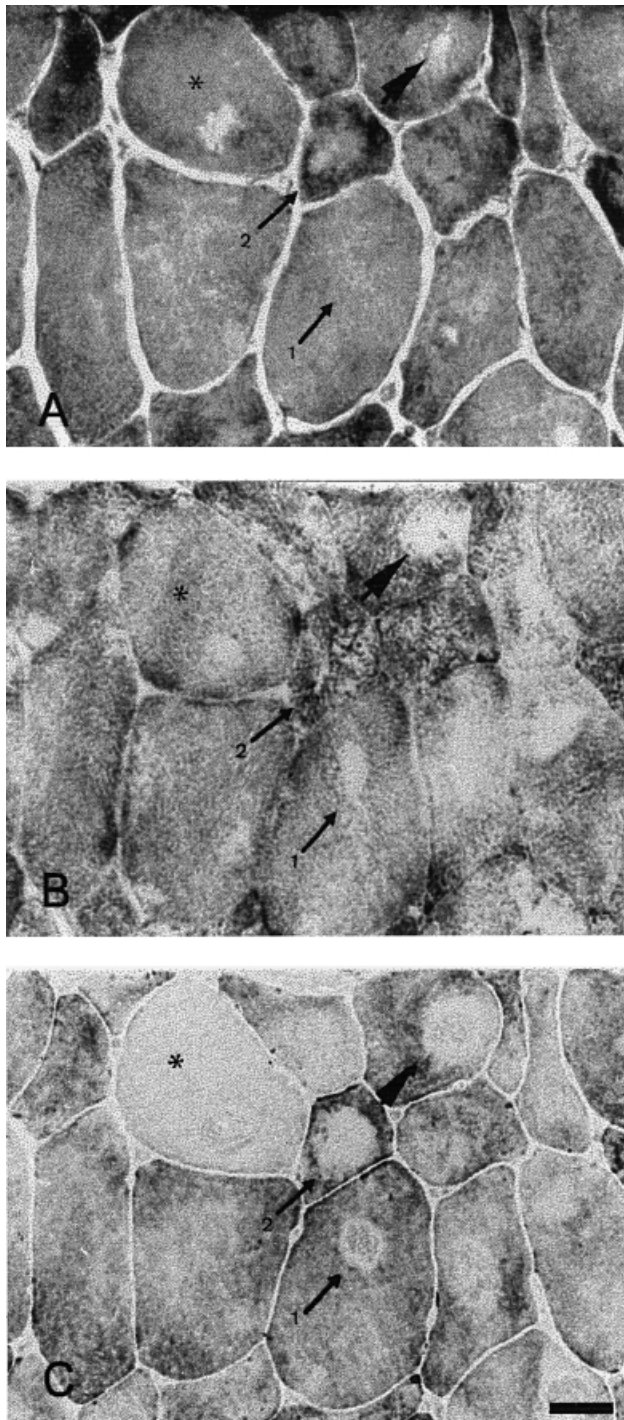


Fig. 1 Muscle histology of a 58-year-old SALS patient. Different staining methods were correlated directly in consecutive sections. Overview illustrating NADHTR (A), SDH (B) and COX (C). Four different staining patterns are present. Asterisk = COX-negative muscle fibre (COX⁻/SDH⁺/NADH⁺); arrow 1 = COX-negative core structure (COX⁻/SDH⁻/NADH⁺); arrow 2 = COX-negative core structure (COX⁻/SDH⁺/NADH⁻); large arrow = COX-negative core structure (COX⁻/SDH⁻/NADH⁻); bar = 17.7 μ m.

The mitochondrial impairment in SALS muscle is related to mtDNA abnormalities

We screened the mtDNA of all patients for the presence of large-scale rearrangements (deletions or duplications) known to be associated with mtDNA diseases, such as with chronic progressive external ophthalmoplegia and Kearns–Sayre syndrome (Holt *et al.*, 1988). *Pvu*II–*Bam*HI double cleavage of the skeletal muscle DNA revealed multiple deletions in one of the 17 patients, as indicated by Southern blots hybridized with a digoxigenin-labelled human mtDNA probe (Fig. 3, lane 4). The normal cleavage pattern with both restriction enzymes resulted in only two fragments of 11.6 and 5.0 kb (lanes 1–3). In one SALS patient sample, six additional bands with lower molecular weights were observed (Fig. 3, lane 4) indicating deletions of 7, 5, 3.5, 2.5 (two) and 2 kb. Furthermore, we quantified the levels of intact mtDNA in our SALS biopsies. The relative amount of intact mtDNA with respect to the nuclear genes can be evaluated from Southern blots of total DNA from skeletal muscle hybridized with a defined mixture of labelled mtDNA and 18S rDNA probes (Tritschler *et al.*, 1992). The chromosomal multicopy 18S rDNA gene serves as a reference marker for the amount of nuclear DNA present in the total DNA sample. In Fig. 4, typical Southern blots from the muscle DNA of three SALS patients (lanes 1–3) are compared with those of two spinal muscular atrophy patients (lanes 4 and 5) and one control (lane 6). These blots show lower mtDNA content in SALS muscle than in control and spinal muscular atrophy muscle. We quantified the degree of mtDNA depletion (mtDNA/18S rDNA ratios) from all SALS patients with ³²P-labelled probes using a phosphoimager. A plot of the mtDNA/18S rDNA ratios versus the citrate synthase activities of all investigated skeletal muscle samples is shown in Fig. 5. It can be seen that the mtDNA/18S rDNA ratios are lower in the individual SALS muscle samples (filled circles) in comparison with the controls (open circles). The average mtDNA/18S rDNA ratio of SALS samples was 1.4 ± 1.0 , which was statistically significantly different from the ratio observed in our control samples: 2.6 ± 1.2 ($P < 0.01$). This difference is unlikely to be due to a reduction in the number of mitochondria as the activity of the mitochondrial marker enzyme citrate synthase was normal. Only in four out of 17 patients were normal mtDNA/18S rDNA ratios observed. In addition, quantification of nuclei in the SALS biopsies revealed an increase in the number of nuclei by a factor of 1.2 ± 0.2 compared with normal controls (mean number of nuclei in controls 31.8 ± 4.1 per $5400 \mu\text{m}^2$ biopsy cross-section in 10 randomly chosen areas; mean number of nuclei in SALS 39.2 ± 7.8 per $5400 \mu\text{m}^2$). This relatively slight increase in nuclear DNA content per muscle biopsy volume would not explain the ~2-fold decrease in the mtDNA/18S rDNA ratio observed in the SALS biopsies.

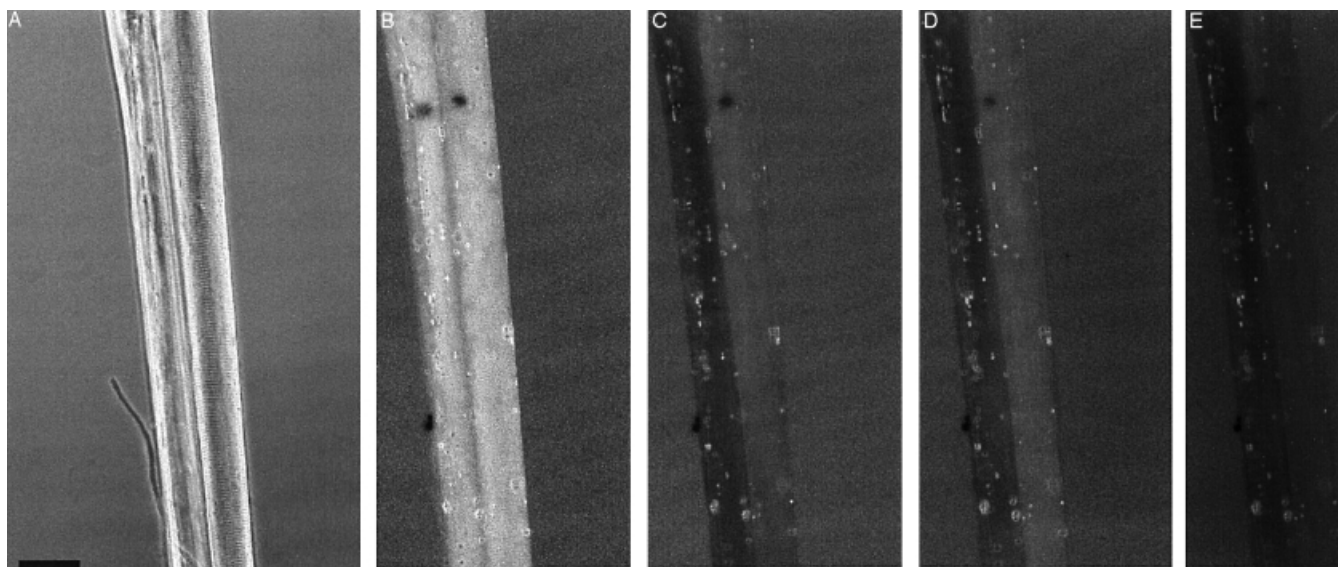


Fig. 2 Digital ratio video fluorescence images of flavoprotein and NAD(P)H fluorescence of a bundle of saponin-permeabilized SALS muscle fibres. A bundle consisting of two saponin-permeabilized muscle fibres of an SALS patient was fixed at both ends in a Heraeus flexiperm chamber and investigated in 300 μ l of buffer for measurements (see Subjects and methods) on the stage of an Olympus IX 70 inverted fluorescence microscope. (A) Phase contrast; (B) digital ratio of flavoprotein and NAD(P)H fluorescence in the endogenous oxidized state; (C) digital ratio image after the addition of 1 mM octanoylcarnitine and 5 mM malate; (D) digital ratio image after the addition of 1 mM ADP; (E) digital ratio image after the addition of 4 mM KCN. Bar = 50 μ m.

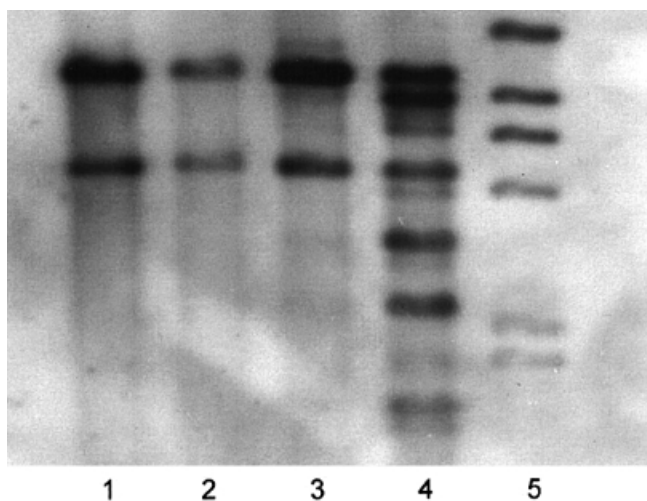


Fig. 3 Southern blots of *Bam*HI-*Pvu*II-digested muscle DNA hybridized with a digoxigenin-labelled human mtDNA probe. A 1 μ g aliquot of total DNA was digested with *Pvu*II and *Bam*HI and hybridized with a human mtDNA probe which recognizes the DNA as a 11.6 kb band (upper band) and a 5.0 kb band (lower band). Lanes 1–4, SALS patients; lane 5, molecular weight standards (*Hind*III-digested lambda DNA), which are, from the top, 23.1, 9.4, 6.6, 4.4, 2.3 and 2.0 kb. In lane 4, six additional bands are seen which correspond to the following deletion lengths: 7, 5 and 2.5 kb of the large (11.6 kb) fragment, and 3.5, 2.5 and 2 kb of the small (5.0 kb) fragment. The presence of these deletions was verified in separate Southern blots of *Pvu*II-digested muscle DNA from this patient which showed three deletions of 7, 5 and 2–3 kb (the different small size deletions of 2–3 kb length were not resolved in these experiments).

Membrane fractions of SALS biopsies show abnormal, low levels of Mn-SOD

The observed mtDNA changes in our SALS patients suggested oxygen radical-mediated mtDNA damage. We therefore examined the amounts of CuZn- and Mn-SOD, which are known to play an important role in detoxification of reactive oxygen species (ROS). The SOD substrate, the superoxide anion radical ($O_2^{\bullet-}$), is the major ROS generated in mitochondria (Skulachev, 1996). In our measurements, we discriminated between soluble and membrane-associated SODs. We therefore analysed the supernatant (containing all cytosolic and mitochondrial matrix enzymes) and the pellet fractions (containing the membrane-bound enzymes) of the muscle homogenates from SALS patients, two spinal muscular atrophy patients (disease controls) and control biopsies. The contents of CuZn- and Mn-SODs in the muscle homogenates determined by ELISA are presented in Table 2. In the supernatant fraction, almost 93% of the total CuZn-SOD was detected. This is in agreement with the cytosolic localization of this enzyme (Fridovich, 1975). On the other hand, for the mitochondrial Mn-SOD, ~40% was associated with the pellet fraction. For the cytosolic CuZn-SOD, no difference was observed between SALS and control muscle. The Mn-SOD levels in pellet fractions of the SALS patients were significantly lower than in the controls and the spinal muscular atrophy patients (Table 2). In a comparison of the individual Mn-SOD levels in the pellet fractions, eight of the SALS patients had lower levels of this enzyme than the lowest value observed in the control group.

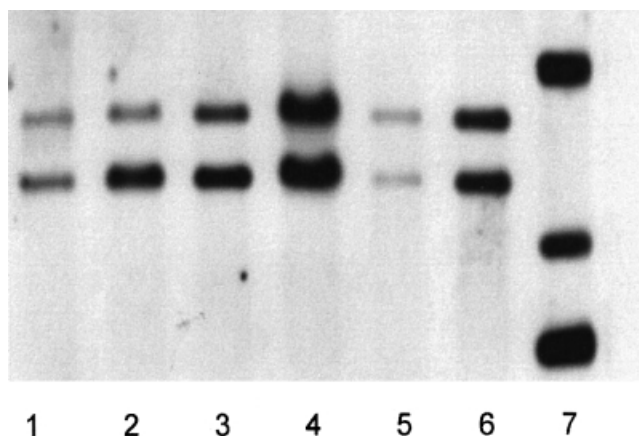


Fig. 4 Southern blots of muscle DNA hybridized with a mixture of digoxigenin-labelled human mtDNA and 18S rDNA probes. A 1 μ g aliquot of total DNA was digested with *PvuII* and hybridized with a mixed probe which recognizes mtDNA as a 16.6 kb band (upper band) and the nuclear 18S rDNA repeat as a 12 kb band (lower band). The mixture of both probes was adjusted to achieve a 1 : 1 ratio of labelling intensities in control samples. Lanes 1–3, SALS patients; lanes 4 and 5, patients with spinal muscular atrophy; lane 6, control; lane 7, molecular weight standards (*HindIII*-digested lambda DNA), which are, from the top, 23.1, 9.4 and 6.6 kb.

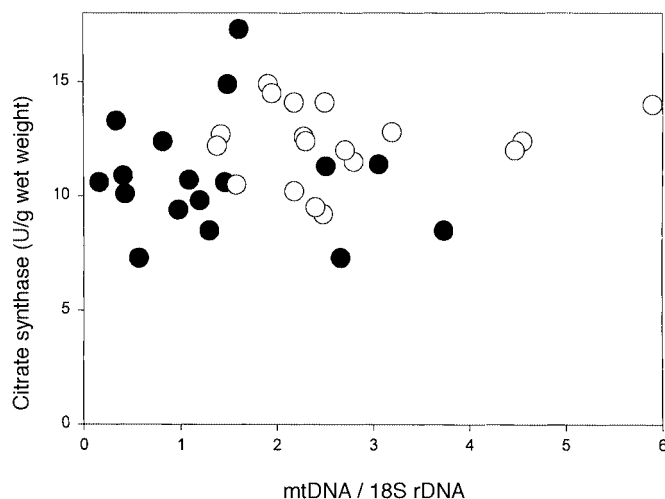


Fig. 5 Plot of mtDNA/18S rDNA ratios versus citrate synthase activities from SALS biopsy samples (filled circles) and controls (open circles). The quantitative ratios of mtDNA/18S rDNA were determined from Southern blots of *PvuII*-cleaved muscle DNA hybridized with a mixture of 32 P-labelled mtDNA and 18S rDNA probes using a phosphoimager.

Discussion

It is known that mitochondria are intrinsically involved in the cellular production of oxygen radicals (Skulachev, 1996) and are believed to play an important part in oxygen radical-mediated cell damage in neurodegenerative diseases (Beal, 1995). In particular, circumstantial evidence for a possible involvement of mitochondria in the pathogenesis of ALS has accumulated. This includes (i) conglomerates of dark abnormal mitochondria in anterior horn neurons of patients

with SALS (Sasaki *et al.*, 1996); (ii) the presence of mitochondrially derived vacuoles in axons and dendrites in the spinal cord of mouse models carrying point mutations in CuZn-SOD (Wong *et al.*, 1995; Mourelatos *et al.*, 1996); (iii) increased oxygen radical damage in post-mortem brain tissue from patients with SALS (Bowling *et al.*, 1993); and (iv) the neuroprotective effect of creatine in mice carrying the G93A human SOD1 mutation (Klivenyi *et al.*, 1999). Recently, we have reported a selective deficiency of NADH:CoQ oxidoreductase in the skeletal muscle of 14 SALS patients (Wiedemann *et al.*, 1998) pointing to a more generalized impairment of mitochondria in SALS. Since respiratory chain-inhibited mitochondria are known to be a powerful source of ROS (Skulachev, 1996) and, in turn, ROS attack both respiratory chain enzymes and mtDNA (Keller *et al.*, 1998), mitochondria can amplify a pre-existing imbalance of oxygen radicals.

In the present study, we have analysed the mitochondria in SALS muscle at multiple molecular levels to examine the detailed nature of the mitochondrial impairment. We demonstrate alterations of mtDNA, including either multiple deletions or depletion of intact mtDNA. These alterations correlate with heterogeneously distributed mitochondrial functional impairment in single muscle fibres as visualized by our fluorescence ratio imaging approach (Kuznetsov *et al.*, 1998). In addition to our earlier study performed with a smaller number of patients, we observed decreased activities of not only NADH:CoQ oxidoreductase but also of COX in the SALS muscle homogenates. We substantiated the latter findings by mitochondrial stains of single muscle fibres showing the presence of COX-negative fibres. Interestingly, the membrane-associated Mn-SOD level was significantly lower in SALS muscle than in controls.

These findings demonstrate the existence of multiple mitochondrial abnormalities in SALS skeletal muscle. However, the observed mitochondrial changes are distinct from the prominent features of classical mitochondrial myopathies such as chronic progressive external ophthalmoplegia or Kearns–Sayre syndrome (Holt *et al.*, 1988). First, although we detected the presence of COX-negative fibres at a frequency of 1–2% of fibres in 11 of 17 patients, we only observed the typical morphological hallmarks of mitochondrial myopathies such as ‘ragged red fibres’ in one patient (Holt *et al.*, 1988; Shoubridge *et al.*, 1990). Secondly, we did not observe a compensatory increase in mitochondrial content (Shoubridge *et al.*, 1990), as indicated by normal citrate synthase activity. Thirdly, in contrast to mitochondrial myopathies, in which the Mn-SOD content is increased (Mitsui *et al.*, 1996), in the present study the membrane-associated Mn-SOD levels were clearly diminished. This may suggest that the underlying mechanism of mitochondrial alterations in SALS muscle and mitochondrial myopathies is distinct. Therefore, the diminished level of membrane-associated Mn-SOD observed in SALS muscle may be a key finding for an SALS-specific pathogenic mechanism, because Mn-SOD is essential for

Table 2 CuZn- and Mn-SOD dismutase levels in ultra-turrax homogenate fractions of skeletal muscle of patients with SALS and spinal muscular atrophy (SMA)

Enzyme	Controls (n = 15)	SMA (n = 2)	SALS (n = 15)
CuZn-SOD supernatant	2410 ± 627	3076 ± 891 NS	2389 ± 289 NS
CuZn-SOD pellet	156 ± 46	151 ± 41 NS	162 ± 33 NS
Mn-SOD supernatant	2254 ± 948	2287 ± 802 NS	1945 ± 792 NS
Mn-SOD pellet	1685 ± 357	2088 ± 602 NS	1208 ± 400 P < 0.01

The enzyme levels, expressed in µg/g wet weight, were determined as described in Subjects and methods. NS = not significant.

ROS detoxification. Since the major site of ROS generation is the mitochondrial respiratory chain (Skulachev *et al.*, 1996), which is localized in the same membrane fraction as membrane-associated Mn-SOD, diminished levels of the enzyme obviously could affect the local concentrations of ROS. Therefore, low membrane-associated Mn-SOD levels could explain the occurrence of multiple mtDNA deletions and depletion of intact mtDNA. Due to the low repair capacity of mtDNA (Shoubridge *et al.*, 1990), stochastic mutations caused by ROS can accumulate and lead to the degradation of damaged molecules. This was shown to occur in Mn-SOD mutant mice exhibiting respiratory chain inhibition and oxidative DNA damage (Melov *et al.*, 1999). A similar phenomenon was also described for yeast mutants lacking the yeast homologue of frataxin which causes Friedreich's ataxia in humans (Wilson and Roof, 1997). In these yeast mutants, the impaired mitochondrial iron transport leads to an accumulation of iron, causing a secondary oxygen radical-mediated mtDNA depletion.

To provide direct proof for the functional impairment of mitochondria within single muscle fibres, we have applied an imaging technique which allows the investigation of mitochondrial function (Kuznetsov *et al.*, 1998). The autofluorescence images of NAD(P)H and fluorescent flavoproteins were detected in individual muscle fibres. The digital ratios of images of both signals are sensitive indicators of mitochondrial function (Mayevsky and Chance, 1982). In the case of respiratory chain inhibition, the flavoprotein/NAD(P)H ratio image of the fibre stays dark even if the respiratory chain is activated by the addition of ADP. Applying this technique, we have observed, in complete agreement with our histochemical studies, a heterogeneous distribution of the mitochondrial defect within the muscle fibre bundles in the majority of investigated SALS patients (11 out of 17). We feel that this imaging technique is a valuable tool for the analysis of mitochondrial dysfunction in skeletal muscle. The results of these investigations are in complete agreement with the occurrence of activity defects of COX in single muscle fibres.

Our results have implications for the pathogenic mechanism of SALS at least in a subgroup of patients. First, the

mitochondrial impairment was not related to age- or denervation-associated muscular changes since the functional impairment of mitochondria (cf. also Wiedemann *et al.*, 1998), the mtDNA alterations and the decreased levels of membrane-associated Mn-SOD (this report) were not observed in spinal muscular atrophy and in controls of similar age. Secondly, our histological investigations indicated that not the muscle fibres with the typical signs of a denervation associated change, i.e. angulated, atrophic fibres or target fibres, showed a specific mitochondrial defect. Thirdly, the finding that the decreased membrane-associated Mn-SOD levels in the SALS biopsies are the possible cause of the observed mtDNA alterations provides a basis to suggest a similar pathogenic mechanism for SALS and FALS [mutations in CuZn-SOD have been shown to be associated with FALS in ~10% of cases (Rosen *et al.*, 1993)]. Impaired ROS detoxification can explain the elevation of lipid and protein peroxidation markers in brain (Bowling *et al.*, 1993) and cerebrospinal fluid (Smith *et al.*, 1998) of patients with SALS. Finally, the neuroprotective effect of creatine administration to mice which carry the G93A CuZn-SOD mutation (Klivenyi *et al.*, 1999) strongly emphasizes that a defect in energy metabolism is of pathogenetic relevance for ALS.

Together, our results support the view that oxygen radicals may cause the observed multiple mitochondrial alterations which seem to be caused by decreased levels of membrane-associated Mn-SOD. This finding may be of relevance for the development of neuroprotective strategies in the treatment of this disease.

Acknowledgements

We wish to thank U. Schneider and P. Rausch (Department of Epileptology, Bonn), K. Kaiser (Department of Neurology, Magdeburg), I. Schellhase (Department of Neuropathology, Magdeburg), and M. Bode and M. Möckel (Department of Neurobiology, Magdeburg) for technical assistance. This work was supported by the BONFOR program of the University of Bonn, a research grant of Aventis Pharma Germany to W.S.K., the Deutsche Gesellschaft für

Muskelkranke DGM e.V., the SFB 387 and BMBF 07 NBL04 (Magdeburg).

References

- Beal MF. Aging, energy and oxidative stress in neurodegenerative diseases. [Review]. *Ann Neurol* 1995; 38: 357–66.
- Bergmeyer HU. *Methoden der enzymatischen Analyse*. 2nd edn. Weinheim: Verlag Chemie; 1970.
- Bowling AC, Schulz JB, Brown RH Jr, Beal MF. Superoxide dismutase activity, oxidative damage, and mitochondrial energy metabolism in familial and sporadic amyotrophic lateral sclerosis. *J Neurochem* 1993; 61: 2322–5.
- Brooks BR. El Escorial World Federation of Neurology criteria for the diagnosis of amyotrophic lateral sclerosis. *J Neurol Sci* 1994; 124 Suppl: 96–107.
- Chiu AY, Zhai P, Dal Canto MC, Peters TM, Kwon YW, Prattis SM, et al. Age-dependent penetrance of disease in a transgenic mouse model of familial amyotrophic lateral sclerosis. *Mol Cell Neurosci* 1995; 6: 349–62.
- Comi GP, Bordoni A, Salani S, Franceschina L, Sciacco M, Prele A, et al. Cytochrome c oxidase subunit I microdeletion in a patient with motor neuron disease. *Ann Neurol* 1998; 43: 110–6.
- Dubowitz V, Brooke MH. *Muscle biopsy. A modern approach*. Philadelphia: W.B. Saunders; 1973.
- Emery AE. Population frequencies of neuromuscular diseases—II. Amyotrophic lateral sclerosis (motor neurone disease). [Review]. *Neuromuscul Disord* 1991; 1: 323–5.
- Fridovich I. Superoxide dismutases. [Review]. *Annu Rev Biochem* 1975; 44: 147–59.
- Holt IJ, Harding AE, Morgan-Hughes JA. Deletions of muscle mitochondrial DNA in patients with mitochondrial myopathies. *Nature* 1988; 331: 717–9.
- Keller JN, Kindy MS, Holtsberg FW, St Clair DK, Yen HC, Germeyer A, et al. Mitochondrial manganese superoxide dismutase prevents neural apoptosis and reduces ischemic brain injury: suppression of peroxynitrite production, lipid peroxidation, and mitochondrial dysfunction. *J Neurosci* 1998; 18: 687–97.
- Klivenyi P, Ferrante RJ, Matthews RT, Bogdanov MB, Klein AM, Andreassen OA, et al. Neuroprotective effects of creatine in a transgenic animal model of amyotrophic lateral sclerosis. *Nature Med* 1999; 5: 347–50.
- Kunz WS, Kuznetsov AV, Schulze W, Eichhorn K, Schild L, Striggow F, et al. Functional characterization of mitochondrial oxidative phosphorylation in saponin-skinned human muscle fibers. *Biochim Biophys Acta* 1993; 1144: 46–53.
- Kuznetsov AV, Mayboroda O, Kunz D, Winkler K, Schubert W, Kunz WS. Functional imaging of mitochondria in saponin-permeabilized mice muscle fibers. *J Cell Biol* 1998; 140: 1091–9.
- Ludolph AC, Hugon J, Dwivedi MP, Schaumburg HH, Spencer PS. Studies on the aetiology and pathogenesis of motor neuron diseases. 1. Lathyrism: clinical findings in established cases. *Brain* 1987; 110: 149–65.
- Mayevsky A, Chance B. Intracellular oxidation–reduction state measured in situ by a multichannel fiber-optic surface fluorometer. *Science* 1982; 217: 537–40.
- Melov S, Coskun P, Patel M, Tuinstra R, Cottrell B, Jun AS, et al. Mitochondrial disease in superoxide dismutase 2 mutant mice. *Proc Natl Acad Sci USA* 1999; 96: 846–51.
- Meyer T, Lenk U, Kuther G, Weindl A, Speer A, Ludolph AC. Studies of the coding region of the neuronal glutamate transporter gene in amyotrophic lateral sclerosis. *Ann Neurol* 1995; 37: 817–9.
- Meyer T, Speer A, Meyer B, Sitte W, Kuther G, Ludolph AC. The glial glutamate transporter complementary DNA in patients with amyotrophic lateral sclerosis. *Ann Neurol* 1996; 40: 456–59.
- Mitsui T, Kawai H, Nagasawa M, Kunishige M, Akaike M, Kimura Y, et al. Oxidative damage to skeletal muscle DNA from patients with mitochondrial encephalomyopathies. *J Neurol Sci* 1996; 139: 111–6.
- Mourelatos Z, Gonatas NK, Stieber A, Gurney ME, Dal Canto MC. The Golgi apparatus of spinal cord motor neurons in transgenic mice expressing mutant Cu,Zn superoxide dismutase becomes fragmented in early, preclinical stages of the disease. *Proc Natl Acad Sci USA* 1996; 93: 5472–7.
- Rosen DR, Siddique T, Patterson D, Figlewicz DA, Sapp P, Hentati A, et al. Mutations in Cu/Zn superoxide dismutase gene are associated with familial amyotrophic lateral sclerosis. *Nature* 1993; 362: 59–62.
- Rothstein JD, Martin LJ, Kuncl RW. Decreased glutamate transport by the brain and spinal cord in amyotrophic lateral sclerosis. *N Engl J Med* 1992; 326: 1464–8.
- Saks VA, Veksler VI, Kuznetsov AV, Kay L, Sikk P, Tiivel T, et al. Permeabilized cell and skinned fiber techniques in studies of mitochondrial function in vivo. *Mol Cell Biochem* 1998; 184: 81–100.
- Sambrook J, Fritsch EF, Maniatis T. *Molecular cloning: a laboratory manual*, Vol. 2. 2nd edn. Cold Spring Harbor (NY): Cold Spring Harbor Laboratory Press; 1989.
- Sasaki S, Iwata M. Ultrastructural study of synapses in the anterior horn neurons of patients with amyotrophic lateral sclerosis. *Neurosci Lett* 1996; 204: 53–6.
- Shoubridge EA, Karpati G, Hastings KE. Deletion mutants are functionally dominant over wild-type mitochondrial genomes in skeletal muscle fiber segments in mitochondrial disease. *Cell* 1990; 62: 43–9.
- Skulachev VP. Role of uncoupled and non-coupled oxidations in maintenance of safely low levels of oxygen and its one-electron reductants. [Review]. *Q Rev Biophys* 1996; 29: 169–202.
- Smith RG, Henry YK, Mattson MP, Appel SH. Presence of 4-hydroxynonenal in cerebrospinal fluid of patients with sporadic amyotrophic lateral sclerosis. *Ann Neurol* 1998; 44: 696–9.
- Spencer PS, Nunn PB, Hugon J, Ludolph AC, Ross SM, Roy DN. Guam amyotrophic lateral sclerosis–parkinsonism–dementia linked to a plant excitant neurotoxin. *Science* 1987; 237: 517–22.

Tritschler H-J, Andreetta F, Moraes CT, Bonilla E, Arnaudo E, Danon MJ, et al. Mitochondrial myopathy of childhood associated with depletion of mitochondrial DNA. *Neurology* 1992; 42: 209–17.

Wiedemann FR, Winkler K, Kuznetsov AV, Bartels C, Vielhaber S, Feistner H, et al. Impairment of mitochondrial function in skeletal muscle of patients with amyotrophic lateral sclerosis. *J Neurol Sci* 1998; 156: 65–72.

Wilson RB, Roof DM. Respiratory deficiency due to loss of mitochondrial DNA in yeast lacking the frataxin homologue. *Nature Genet* 1997; 16: 352–7.

Wong PC, Pardo CA, Borchelt DR, Lee MK, Copeland NG, Jenkins NA, et al. An adverse property of a familial ALS-linked SOD1 mutation causes motor neuron disease characterized by vacuolar degeneration of mitochondria. *Neuron* 1995; 14: 1105–16.

Received October 11, 1999. Revised December 21, 1999.

Accepted January 24, 2000